Available online at www.sciencedirect.com
ScienceDirect
C. R. Geoscience 340 (2008) 211–222
COMPTES RENDUS GEOSCIENCE
http://france.elsevier.com/direct/CRAS2A/

Geomaterials

Archean inheritances in the pyroxene–amphibole-bearing gneiss of the Méiganga area (Central North Cameroon): Geochemical and $^{207}Pb/^{206}Pb$ age imprints

Alembert Alexandre Ganwa [a,b], Wolfgang Frisch [b,*], Wolfgang Siebel [b], Georges Emmanuel Ekodeck [c], Cosmas Kongyuy Shang [b], Vincent Ngako [d]

[a] *Department of Earth Sciences, University of Ngaoundéré, P.O. Box 454 Ngaoundéré, Cameroon*
[b] *Department of Earth Sciences, University of Tubingen, Sigwartstr, 10, D72076 Tübingen, Germany*
[c] *Department of Earth Sciences, University of Yaoundé, P.O. Box 872 Yaoundé, Cameroon*
[d] *Institute of Mining and Geological Research (IRGM), Yaoundé, P.O. Box 4110, Cameroon*

Received 21 July 2006; accepted after revision 18 December 2007
Available online 5 March 2008

Presented by Ždenek Johan

Abstract

The Méiganga area is located in the central part of the Panafrican belt of Cameroon. This region is underlain by a granitic and gneissic basement, crosscut, and covered by basaltic and phonolitic rocks. To the southwest of Méiganga, the pyroxene-and-amphibole-bearing gneiss shows the geochemical characteristics of Archean TTG (tonalite—trondhjemite—granodiorite) associations. The studied samples show LREE enrichment relative to the HREE (La_N/Yb_N = 7–28). This pattern of the REE, particularly the concentration of Y and Yb allowed us to consider some samples as derived from an Archean crust. Cathodoluminescence pictures of zircon crystals from the gneiss reveal magmatic oscillatory zoning with inherited cores. Age determinations employing the $^{207}Pb/^{206}Pb$ single-zircon evaporation method yielded Late Archean (~2.6 Ga) to Palaeoproterozoic (~1.7 Ga) ages. Ages around 2.0 Ga are interpreted to be close to the crystallization age, while the older ages might represent mixing ages, i.e., mixtures between a Palaeoproterozoic magmatic domain and an inherited Archean core. This study discusses the imprints of Archean crust inheritances on the pyroxene–amphibole-bearing gneisses of the Méiganga area. ***To cite this article: A.A. Ganwa et al., C. R. Geoscience 340 (2008).***

Résumé

Héritages archéen dans les gneiss à pyroxène et amphibole de Méiganga (Centre Nord du Cameroun) : empreintes géochimiques et d'âge $^{207}Pb/^{206}Pb$. La région de Méiganga est située dans la partie centrale de la chaîne panafricaine du Cameroun. Elle est constituée d'un socle granitique et gneissique, recouvert ou traversé par des formations basaltiques et phonolitiques. Les gneiss à pyroxène et amphibole au sud-ouest de Méiganga montrent des caractères géochimiques voisins de ceux des TTG (tonalite, trondhjémite, granodiorite) archéennes. Les échantillons étudiés montrent un enrichissement en LREE par rapport aux HREE (La_N/Yb_N = 7–28). Cette distribution des terres rares, et en particulier les concentrations en Y et en Yb, ont permis de définir certains échantillons comme provenant d'une croûte archéenne. La cathodoluminescence révèle que leurs zircons

* Corresponding author.
E-mail address: w.frisch@uni-tuebingen.de (W. Frisch).

1631-0713/$ – see front matter
doi:10.1016/j.crte.2007.12.009

ont une zonation magmatique oscillatoire, avec des cœurs hérités. Les âges déterminés par la méthode d'évaporation $^{207}Pb/^{206}Pb$ sur monozircon sont tardi-archéens (2,6 Ga) à paléoprotérozoïques (1,7 Ga). Les âges autour de 2 Ga sont proches de l'âge de cristallisation, alors que les âges plus anciens résulteraient d'un mélange, par exemple, entre des domaines de zircon paléoprotérozoïque magmatique et le cœur archéen hérité. Le présent travail met en évidence les empreintes de l'héritage d'une croûte archéenne dans les gneiss à pyroxène et amphibole de la région de Méiganga. ***Pour citer cet article : A.A. Ganwa et al., C. R. Geoscience 340 (2008).***

Keywords: Archean inheritances; Palaeoproterozoic; TTG; Panafrican belt; Pyroxene–amphibole gneiss; $^{207}Pb/^{206}Pb$ zircon evaporation method; Meiganga; Cameroon

Mots clés : Héritage archéen ; Paléoprotérozoïque ; TTG ; Gneiss à pyroxène et amphibole ; Méthode d'évaporation $^{207}Pb/^{206}Pb$ sur zircon ; Méiganga ; Cameroun

1. Introduction

Cameroon is underlain by Cretaceous to Recent volcanosedimentary formations and by a plutonometamorphic basement. This basement comprises the northern edge of the Archean Congo craton to the south (Ntem complex) and the Panafrican formations that occupy more than the half of the national territory (Fig. 1). Many petrographic, chemical, isotopic, and geochronological studies [29,46,54] were carried out in the Ntem complex. The Panafrican fold belt, defined in the 1960s and 1970s [5,16], is constituted by Neoproterozoic and Palaeoproterozoic formations that have been reworked during the Panafrican orogeny. During the 1980s and 1990s, petrographic, structural, chemical and geochronological studies were carried out in the northern [31,33,34,44,59] and southern parts [12,28,36,37,42,53] of the Panafrican fold belt of Cameroon. The northern part is made up of juvenile Neoproterozoic and Palaeoproterozoic material (660- to 580-Ma-old granitoids, 800-Ma-old orthogneisses) without contribution of Archean materials. The southern part is made up of 620-Ma-old schists and gneisses, and ∼700-Ma-old volcanic derivatives; these rocks were derived from juvenile materials contaminated by Palaeoproterozoic crust. Since the end of the 1990s, attention also focused on the geodynamic evolution of the fold belt [7,32,34,38,52,57].

The models of continental crust evolution are ill defined, since they all depend on poorly known parameters concerning the proportion of Archean material in the crust [1]. Indeed this assessment is difficult, because the segments of the various orogenies consist of ancient recycled crust associated with juvenile crust issued from the mantle. The present study is aimed at identifying Archean material in the Méiganga area (central Cameroon), which is composed of a 2.1-Ga-old metamorphic basement reworked during the Pan-African orogeny. The latter is characterized by the emplacement of granites within the 650–550-Ma time interval. A two-step approach has been used, based on:

(a) the behaviour of the major elements, Y and REE, which allows one to characterize the Archean crust composed of a tonalite—trondhjemite—granodiorite (TTG) association;
(b) after establishing the zircon typology through cathodoluminescence, $^{207}Pb/^{206}Pb$ dating on single zircon crystals, revealing the different phases of zircon growth, which are assumed to correspond to successive orogenies.

2. Geological setting

The Méiganga area (Fig. 2) belongs to the Adamawa region, in the central part of the Panafrican fold belt of Cameroon; it is underlain by syn-tectonic, late-tectonic, and post-tectonic granitoids [22,58], hosted in metamorphic formations. The granitoids are partially covered by basaltic lavas or crosscut by phonolitic domes [35]. Early data from the granitoids yielded ages in the 500–600-Ma range [4]. Recent Th–U–Pb monazite dating in the Ngaoundéré region yielded $\sim 615 \pm 27$ Ma and $\sim 575 \pm 8$ Ma for the emplacement of biotite–muscovite granite and biotite granite, respectively [56]. The metamorphic host rocks comprise metasediments and ∼2.1-Ga-old orthogneisses, which were reworked during the Panafrican orogeny [58]. U–Pb dating on metaigneous rocks (hornblende–biotite gneiss) of the Mbé region to the north of Ngaoundéré gives an age around 2.1 Ga [43]. In the Méiganga area, the basement comprises also banded amphibolites, amphibole biotite gneisses, and pyroxene amphibole gneisses. Banded amphibolites consist of quartz–feldspar layers alternating

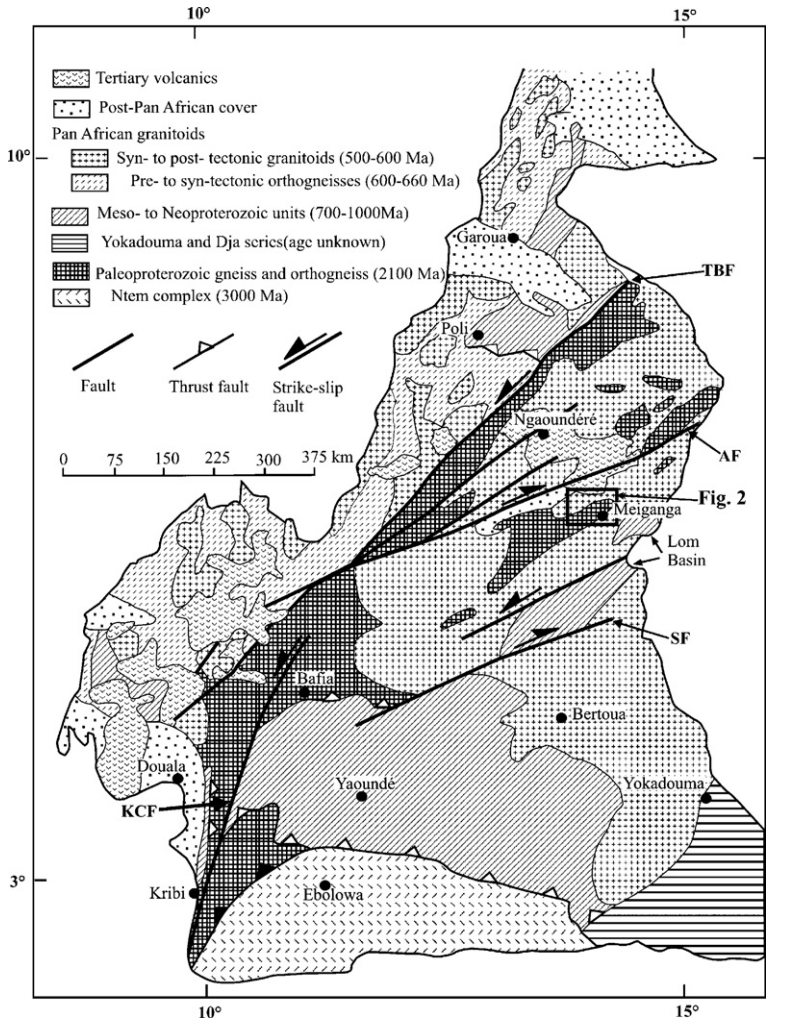

Fig. 1. Geological map of Cameroon (after [58]) showing the major lithotectonic units. **KCF**, Kribi–Campo fault; **AF**, Adamaoua fault; **SF**, Sanaga fault; **TBF**, Tcholliré–Banyo fault.

Fig. 1. Carte géologique du Cameroun (d'après [58]) montrant les grands ensembles lithologiques. **AF**, faille de l'Adamaoua ; **KCF**, faille de Kribi–Campo ; **SF**, faille de la Sanaga ; **TBF**, faille de Tcholliré–Banyo.

with amphibole-rich layers; amphibole–biotite and pyroxene–amphibole gneisses are made up of quartz, plagioclase, K-feldspar, biotite, hornblende, pyroxene, and accessory minerals (sphene, zircon, and apatite).

The studied samples were collected to the southwest of Méiganga, around Kalaldi, and to the southeast of Doua (cf. Fig. 2). The samples are pyroxene–amphibole-bearing gneisses, with a fine- to medium-banded structure. The banded structure is often reinforced by migmatisation, the melts being characterized by light quartzofeldspatic bands. The gneisses contain layers of amphibolite and sometimes enclaves of massive mafic rocks. Under the microscope, they show grano-nematoblastic to granoblastic structure and are made up of pyroxene, amphibole, biotite, quartz, feldspar, opaque minerals, and accessory minerals (apatite, titanite, and zircon). Pyroxene is xenomorphic in shape and often rimmed by secondary hornblende. Amphibole is a green hornblende, associated with dark brown flakes of biotite, which are often deformed. The rocks contain epidote (probably derived from the anorthite component of plagioclase), and biotite is partly transformed into chlorite. Plagioclase is 0.15 to 10 mm long, with oscillatory zoning; it is often affected by fractures. Quartz forms polycrystalline aggregates and shows undulatory extinction. It is generally an interstitial mineral.

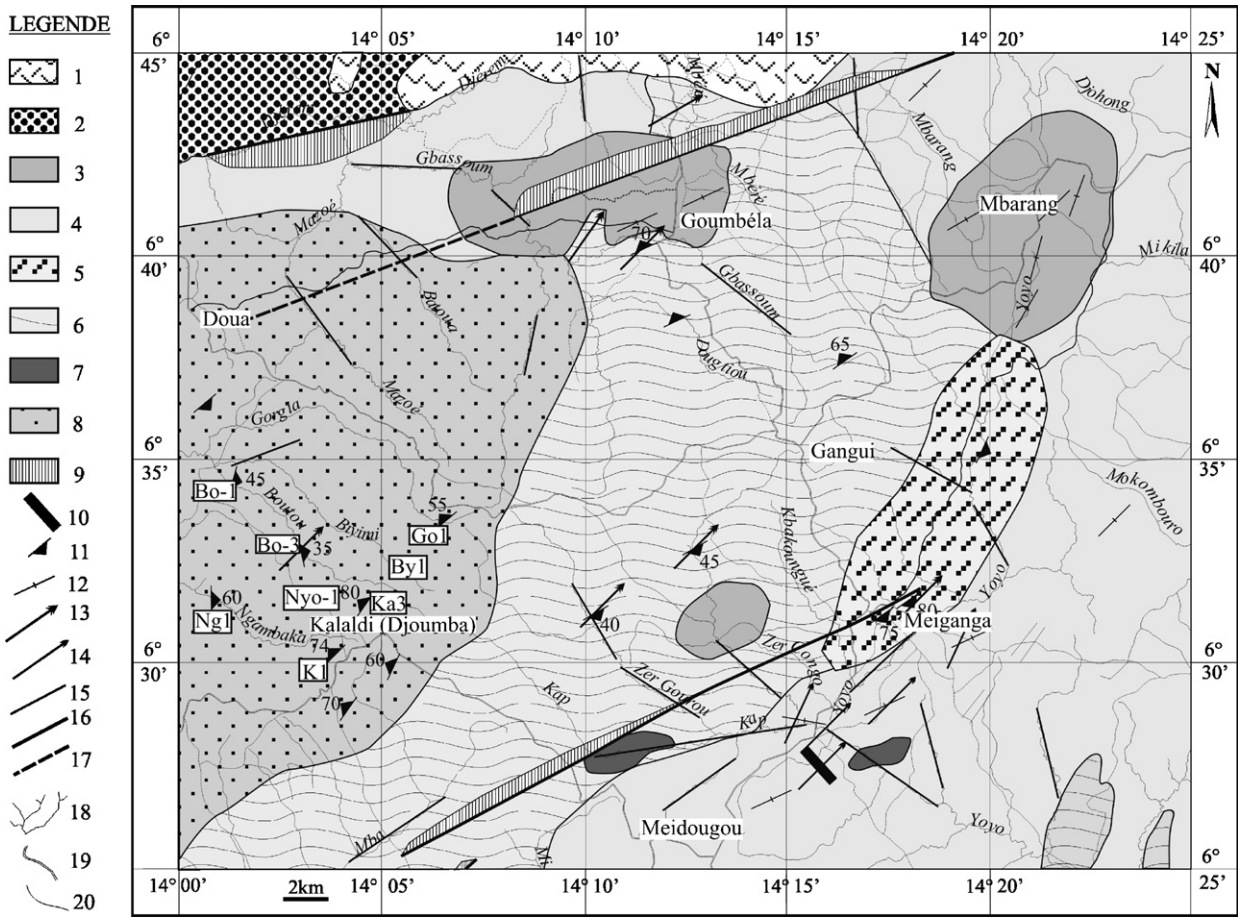

Fig. 2. Geological map of the Méiganga area (after [13]) showing the position of the studied samples around the Kalaldi village: (**1**) basalt, (**2**) conglomerate, (**3**) biotite–muscovite granite, (**4**) pyroxene–amphibole–biotite granite, (**5**) banded amphibolite, (**6**) amphibole–biotite gneiss, (**7**) amphibolite, (**8**) pyroxene–amphibole gneiss, (**9**) mylonite, (**10**) dolerite, (**11**, **12**) schistosity, (**13**, **14**) lineations, (**15**) fractures, (**16**) fault, (**17**) supposed fault, (**18**) rivers, (**19**) road, (**20**) path.

Fig. 2. Carte géologique de la région de Méiganga (d'après [13]) montrant la position des échantillons analysés autour du village Kalaldi. (**1**) basalte, (**2**) conglomérat, (**3**) granite à biotite et muscovite, (**4**) granite à pyroxène, amphibole et biotite, (**5**) amphibolite rubanée, (**6**) gneiss à amphibole et biotite, (**7**) amphibolite, (**8**) gneiss à pyroxène et amphibole, (**9**) mylonite, (**10**) dolérite, (**11**, **12**) schistosités, (**13**, **14**) linéations, (**15**) fractures, (**16**) faille, (**17**) faille supposée, (**18**) cours d'eau, (**19**) route, (**20**) piste.

3. Analytical methods

Major and trace elements were analysed by X-ray fluorescence (XRF) at the University of Tubingen. Rare-earth elements were analysed by Inductively Coupled Plasma–Atomic Emission Spectrometry (ICP–AES) at the CRPG ('Centre de recherches pétrographiques et géochimiques', Vandœuvre-lès-Nancy, France). Analytical uncertainties are estimated at $\pm$ 1% for major elements and 5–10% for most trace elements.

Zircon grains were separated from 200–63-μm sieved rock fractions by standard separation techniques (milling, wet shaking table, magnetic and heavy liquid separation) and finally handpicked under the binocular microscope. Cathodoluminescence images were performed on an electronic microscope LEO Model 1450 VP (variable pressure) 4-Quadrant BSE-Detector working with an accelerating voltage of 10 kV.

For single-zircon Pb evaporation, whole zircon grains were analysed using a double Re filament configuration. Principles of the evaporation method are described in [19,20]. Measurements were done using a Finnigan MAT 262 mass spectrometer equipped with a MassCom ion counter at the University of Tubingen. The linearity of the amplifier was controlled by the NBS standard 981. All $^{207}Pb/^{206}Pb$ ratios were corrected for common Pb according to [9], and the error for a single

Table 1
Chemical data of the pyroxene–amphibole-bearing gneiss samples

Tableau 1
Données d'analyse chimique des échantillons du gneiss à pyroxène et amphibole

Samples	By1	Go1	Ka1	Ka3a	Nyo-1	Ng-1	Bo-3	Bo-1
SiO_2	58.84	69.30	60.72	64.37	67.05	66.51	67.63	65.14
TiO_2	0.84	0.46	0.65	0.71	0.83	0.65	0.74	0.55
Al_2O_3	16.66	15.04	16.08	15.95	13.73	15.40	13.64	15.81
Fe_2O_3	8.17	4.07	6.66	6.34	6.85	5.30	6.19	5.44
MnO	0.13	0.04	0.11	0.12	0.09	0.07	0.09	0.08
MgO	2.80	1.36	3.22	2.06	1.51	1.30	1.59	2.30
CaO	5.80	2.68	6.11	5.29	4.00	4.97	3.47	4.27
Na_2O	5.43	3.58	4.20	4.17	3.43	4.16	3.22	4.05
K_2O	1.28	3.46	1.45	0.91	2.21	1.64	3.24	2.02
P_2O_5	0.19	0.19	0.20	0.19	0.26	0.21	0.26	0.19
LOI	0.56	0.59	1.02	0.64	0.29	0.32	0.53	0.69
Sum	100.93	101.15	100.56	100.96	100.49	100.73	100.84	100.74
$Na_2O + K_2O$	6.71	7.04	5.64	5.08	5.65	5.80	6.46	6.06
Na_2O/K_2O	4.25	1.03	2.90	4.58	1.55	2.54	1.00	2.01
A/CNK	0.80	1.04	0.82	0.91	0.90	0.87	0.90	0.95
Mg#	40	40	49	39	30	33	34	46
Ba	748	2270	305	684	1377	897	1309	1079
Co	22.6	9.2	55.9	35.4	16.1	13.3	13.4	14.3
Cr	146	273	67	108	14	21	20	33
Ni	86.2	121	56.6	61.4	1.6	9.9	5.8	18.6
Rb	28.4	92.9	49.6	37.9	60.3	31.1	92.1	66.7
Sr	659	495	389	619	242	513	249	389
V	138.8	47.3	105.8	96.4	88.4	73.2	80	82.1
Y	25.5	7.2	23	23.3	31.7	14.9	42.8	15.9
Zn	77.4	37.3	46	46.7	60.5	31.8	56.8	51.4
Zr	228	173	143	211	232	188	269	184
K	10600	28746	11995	7554	18378	13614	26870	16743
La	43	104	40	43	28	40	59	39
Ce	51	199	55	46	60	49	129	68
Pr	28.9	56.3	6.51	5.25	29.8	27.8	55.4	6.30
Nd	5.3	11.1	30.1	24.7	6.2	4.9	7.7	25.4
Sm	1.9	1.8	5.5	4	1.1	1.5	1.2	6.2
Eu	2	—	1.3	1.7	2.7	1	3.6	1.3
Gd	19.7	12.9	4.52	3.65	13.3	10.9	19.8	2.69
Tb	8.6	39.3	0.66	0.55	4.6	10.9	14.9	0.36
Dy	0.4	4.4	3.75	3.19	—	3.2	—	1.92
Ho	19.2	—	0.70	0.62	—	—	18.3	0.34
Er	373	309	2.01	1.75	305	438	292	0.91
Tm	0.04	0.19	0.31	0.25	0.25	0.06	0.37	0.13
Yb	21.5	8.93	2	1.8	7.09	3.41	11.08	0.72
Lu	14.47	—	0.32	0.24	7.63	27.38	5.81	0.12
Hf	25.8	68.75	3.57	4.62		34.4		3.93
Ta			0.97	0.72				0.19
W			341	188				7.76
Pb			10.6	14.3				5
Th			2.3	5.1				3.6
U			—	0.4				2.8
Nb			—	—				—
Be			1.461	1.29				1.15
Cs			0.51	0.79				0.30
Cu			38.3	45.1				22.4
Ga			20.7	18.4				19.7
Ge			1.31	1.08				0.99
Mo			—	1.28				—
Sn			1.81	0.92				0.99

Table 1 (*Continued*)

Samples	By1	Go1	Ka1	Ka3a	Nyo-1	Ng-1	Bo-3	Bo-1
K/Rb			242	199				251
Rb/Sr			0.13	0.06				0.17
Th/U			13.62	12.75				1.29
La_N/Yb_N			0.77	16.27				22.02
Eu/Eu*			16.9	1.31				0.94
Sr/Y				26.5				24.5

zircon age was calculated after [50]. Repeated measurements on natural zircon from Phalaborwa, South Africa [21], and from zircon standard 91500 of 'Kuehl Lake' (Canada) [63] were performed for geologically realistic age and error treatment [8]. The results were similar to those obtained by previous authors [21,63].

4. Geochemical characterization of TTG association in the Méiganga area

TTGs are intermediate to acid rocks ($SiO_2 > 56\%$) of andesite/diorite, dacite/granodiorite or rhyolite/granite type. The studied samples are intermediate to felsic, with 58% to 69% SiO_2 (Table 1). The Al_2O_3 concentration varies between 13% and 17%. The K_2O concentration increases with increasing SiO_2, from 0.90% to 3.5%. The studied gneiss displays a medium- to high-K calc-alkaline character [14,23]. The ASI (A/CNK = $[Al_2O_3/(CaO + Na_2O + K_2O)$ mol%]) indicates metaluminous composition, except for the sample Go-1, with ASI = 1.04. However, ASI values ≤ 1.1 point to an I-type character (e.g., [62]) for these samples. The normative An–Ab–Or and Q–Ab–Or diagrams (Fig. 3a and b) show the studied samples in comparison with the Ebolowa TTG [29] and Sangmelima granodiorite [27] in the Archean Ntem craton; the majority of the samples portray a trondhjemitic character, like the Ebolowa TTG, while three samples show a calc-alkaline character similar to that of the Sangmelima granodiorite. The ferromagnesian oxides content ($Fe_2O_{3Total} + MgO + TiO_2$) varies from 6% to 12%. $Mg\#[Mg^{2+}/(Mg^{2+} + Fe_{Total}) \times 100$, with Fe_{Total} as $Fe^{2+}]$ varies from 30 to 49, with a general decrease with increasing SiO_2. Although K/Rb ratios (199–438) are higher that those reported by [10], similar values are known in many Archean cratons, among which are the Congo craton [46,47], the Antarctic craton [49], and the Sino-Korean craton [15]. The primordial mantle-normalized multi-element diagram [26] (Fig. 4a) shows a pattern similar to the Sangmelima TTG with a negative Ta anomaly. The U content (0–4.4 ppm) is higher than in the Sangmelima charnockites (mean 0.5 ppm) [47], and the Ebolowa potassic granitoids (mean 0.87 ppm) [55]. The $[La_N/Yb_N]$ ratios are between 7 and 28 (cf. Table 1). The samples show slight negative to positive Eu anomalies (Eu/Eu* = 0.76 to 1.31).

The main characteristic of Archean crust is an extremely low content in Y and heavy REE due to partial fusion of a source containing garnet as a residual phase. Accordingly, TTGs usually display Y and Yb concentrations less than 10 and 1 ppm, respectively, which is two to three times less than in normal calc-alkaline rocks. The chondrite-normalized REE patterns [25] (Fig. 4b) of representative samples do not reveal any significant slope from Dy to Lu for samples Ka3 and Ka1; accordingly, this feature permits to conclude that these samples do not belong to TTGs. In contrast, a significant slope from Dy to Lu and low Yb concentration (<1 ppm) are observed for sample Bo-1, showing that this sample is probably a TTG. The Sr/Y ratios for samples Nyo-1, By1 and Bo-3 are less than 30 (7.63, 25.8 and 5.81), the Yb and Y contents greater than 1 and 10 ppm, respectively; samples Go1 and Ng-1 portray Sr/Y ratios of more than 30 and Yb contents of 1 ppm or below. Nyo-1, By1 and Bo-3 cannot be regarded as TTGs, while Go1 and Ng-1 can be.

5. $^{207}Pb/^{206}Pb$ geochronology by evaporation on single zircon crystals

The internal structure of zircon grains was examined in sample Bo-1, a pyroxene–amphibole-bearing gneiss. Fig. 5 shows pictures of representative grains. The BSE (backscattered electron) images of the polished surfaces (indicated with letter a) are light grey (a1) to grey (a4). The zircon grains are fractured, indicating that they have been affected by brittle deformation. They are euhedral (a2) to subhedral (a4) in shape. Zircon grains b1 and b4 show highly luminescent cores without oscillatory zonation, surrounded by less luminescent and slightly zoned rims. The contact between the two parts is irregular and the external part tends to extend into the core. Zircon b2 is free of a core and shows euhedral oscillatory zoning. Zircon b3 has a

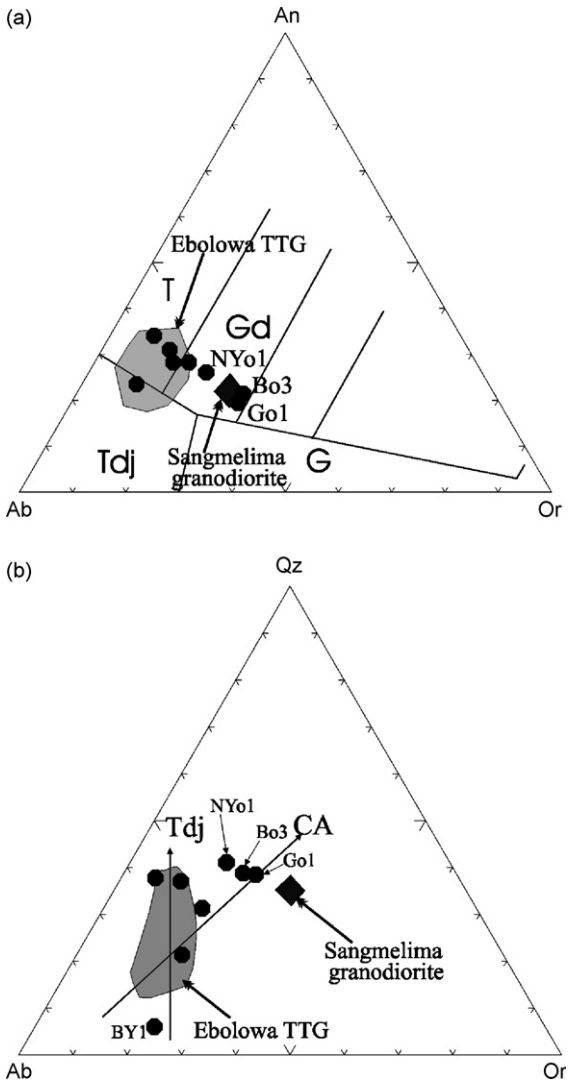

Fig. 3. (**a**) Normative An–Ab–Or classification from O'Connor [39] of studied gneiss in comparison with Ebolowa TTGs [29] and Sangmelima granodiorite [27]. (**b**) Q–Ab–Or normative diagram of Barker and Arth [3] showing the trondhjemitic character of five samples and the calc-alkaline character of three samples (compared with Ebolowa TTG [29] and Sangmélima granodiorite [27]).

Fig. 3. (**a**) Classification des gneiss étudiés dans le diagramme An–Ab–Or de O'Connor [3], comparé aux TTG d'Ebolowa [29] et la granodiorite de Sangmelima [27] (zones grisé clair et grisé sombre. (**b**) Q–Ab–Or normatif d'après Barker et Arth [3], montrant le caractère trondhjémitique de cinq échantillons et calco-alcalin de trois échantillons (zone en grisé clair : TTG d'Ebolowa [29] ; zone en grisé sombre : granodiorite de Sangmelima [27]).

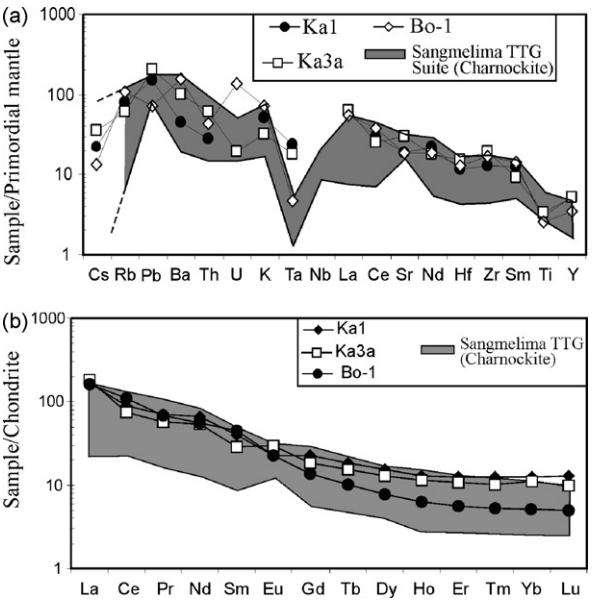

Fig. 4. (**a**) Primordial mantle-normalized spidergrams of the studied gneiss in comparison with the Sangmelima TTGs [48]; normalisation values are from [26]. G = granite ; Gd = granodiorite ;Tdj = trondhjemite ; TTG = tonalite, trondhjemite, granodiorite. (**b**) Chondrite-normalized REE patterns (normalized values are from [25]), in comparison with the Sangmelima TTGs [48].

Fig. 4. (**a**) Diagramme multiélément normalisé au manteau primitif des gneiss étudiés, en comparaison avec les TTG de Sangmélima [48] ; les valeurs de normalisation sont issues de [26]. G = granite ; Gd = granodiorite ; Tdj = trondhjemite ; TTG = tonalite, trondhjémite, granodiorite. (**b**) Spectre des terres rares normalisées à la chondrite (les valeurs de normalisation sont issues de [25]), en comparaison avec les TTG de Sangmélima [48].

well-developed euhedral, oscillatory-zoned core, surrounded by a less luminescent rim. Zircon b5, in contrast, shows a dark core with a rounded shape, and a less luminescent and less expressed oscillatorily zoned rim. Dark cores in zircon were described in high-grade gneiss terranes and reveal high content in U [40]. In the rims of the zircons b4 and b5, the zonation seems to blot out; this can be related to the differential absorption of contaminants during crystallisation [61] or to the influence of deformation [45]. The euhedral oscillatory zonation of the studied zircons is indicative of their magmatic origin.

The results of evaporation of five representative zircon grains of sample Bo-1 are presented in Table 2. The Th/U ratios were calculated using the measured $^{208}Pb/^{206}Pb$ ratios and the apparent $^{207}Pb/^{206}Pb$ dates. The Th/U ratios are generally high and vary from one heating step to another of the same zircon grain, and from one grain to another. This variation is due to the magmatic growth of the zircon, and reflects the magma evolution during zircon growth [17,18]. The Th/U ratios, which vary from 1.3 to 2.7, display no correlation with the heating temperature; they can be compared with the range of values yielded by zircons from the Sangmelima granodiorite [48]. The Th/U ratios could

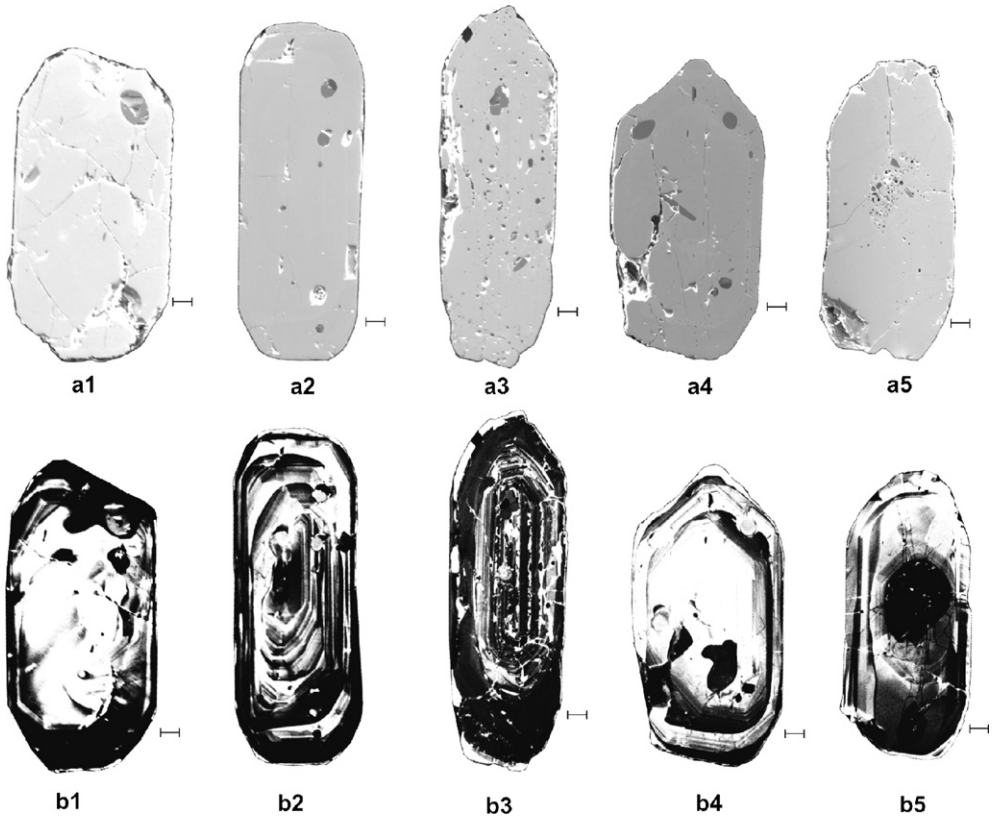

Fig. 5. BSE images (**a**) and cathodoluminescence images (**b**) of representative zircon crystals of the studied gneiss (sample Bo-1).

Fig. 5. Images BSE (**a**) et cathodoluminescence (**b**) de quelques zircons représentatifs du gneiss étudié (échantillon Bo-1).

Table 2
Zircon evaporation data including radiogenic $^{207}Pb/^{206}Pb$ ratios and corresponding ages for the studied gneiss (sample Bo-1)

Tableau 2
Données d'évaporation du zircon avec les rapports $^{207}Pb/^{206}Pb$ radiogénique et les âges correspondants du gneiss étudié (échantillon Bo-1)

Sample and zircon number (a,b,c = temp. step	Evap. Temp °C	No. of ratio	U/Th ratio	$^{206}Pb/^{208}Pb$ ratio	$^{204}Pb/^{206}Pb$ ratio	$^{207}Pb/^{206}Pb$ isotope ratio	$^{207}Pb/^{206}Pb$ age (Ma) 2σ error
1–1a	1400	88	1.46	4.89	0.000065	0.110869 ± 0.000100	1813.7 ± 3.4
1–1b	1430	96	1.87	6.24	0.000069	0.104847 ± 0.000094	1711.7 ± 3.4
1–1c	1460	70	1.97	6.58	0.000067	0.103344 ± 0.000147	1685.0 ± 4.0
1–2a	1410	114	2.00	7.21	0.000239	0.159781 ± 0.000284	2453.4 ± 4.3
1–2b	1440	114	1.87	6.71	0.000239	0.165466 ± 0.000164	2512.3 ± 3.4
1–2c	1470	114	1.64	5.84	0.000239	0.162137 ± 0.000144	2478.2 ± 3.3
1–3a	1380	114	2.45	8.36	0.000019	0.157660 ± 0.000145	2430.7 ± 3.4
1–3b	1410	36	2.10	7.17	0.000014	0.164673 ± 0.000209	2504.3 ± 3.7
1–3c	1435	152	1.41	4.84	0.000010	0.174236 ± 0.000195	2602.6 ± 13.5
1–4a	1380	114	1.28	4.34	0.000337	0.135458 ± 0.000195	2170.0 ± 4.0
1–4b	1400	113	2.70	9.17	0.000153	0.143879 ± 0.000117	2274.5 ± 3.3
1–4c	1420	70	2.51	8.55	0.000103	0.153723 ± 0.000314	2387.8 ± 4.6
1–5a	1380	111	1.44	5.11	0.000253	0.154660 ± 0.000251	2398.2 ± 4.1
1–5b	1400	106	1.65	5.67	0.000051	0.165629 ± 0.000177	2514.0 ± 3.5
1–5c	1430	112	1.70	6.00	0.000165	0.172099 ± 0.000279	2578.2 ± 4.0

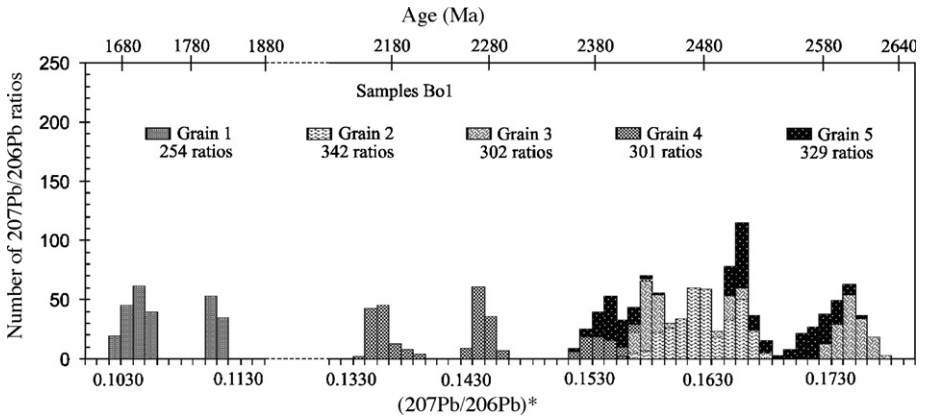

Fig. 6. Histogram showing the distribution of radiogenic $^{207}Pb/^{206}Pb$ ratios obtained from evaporation of zircons from pyroxene-amphibole gneiss (sample Bo-1).

Fig. 6. Histogramme montrant la distribution des rapports $^{207}Pb/^{206}Pb$ obtenus par évaporation des zircons du gneiss à pyroxène et amphibole (échantillon Bo-1).

be influenced by Th-rich inclusions; therefore, the inclusions revealed by the polished section of zircons (cf. Fig. 5) may be Th-rich minerals such as thorite ($ThSiO_4$) or thorianite [$(Th,U)O_2$]. The $^{204}Pb/^{206}Pb$ ratios are less than 0.0001 in seven steps, and 0.001 in one step. The $^{207}Pb/^{206}Pb$ ratios vary from 0.104847 ± 094 to 0.174236 ± 195, the corresponding ages range from ~1.7 Ga (Palaeoproterozoic) to ~2.6 Ga (Late Archean) (Fig. 6). There is no good age reproducibility either between different heating steps of the same grain or between different grains. This is probably due to the presence of cores in many zircons of the studied sample.

6. Discussion and conclusion

The Méiganga area is underlain by granitic and metamorphic rocks comprising pyroxene–amphibole-bearing orthogneisses. These are mesocratic to leucocratic rocks with medium- to high-potassic calc-alkaline character. Their normative composition and the decrease of the Mg# relative to the increase of SiO_2 (Fig. 7) show affinities with many TTGs: Sangmelima charnockites [47], Ebolowa granitoids [55] from the Congo craton, and other <3.0-Ga-old TTGs [51]. They exhibit negative anomalies in Ta and Ti, and are enriched with LREE with respect to the HREE (cf. Fig. 4a and b).

The zircons of the gneisses are euhedral, with oscillatory zonation. They show U-rich cores (e.g., [40]) and have been influenced by subsequent deformation [45]. The $^{207}Pb/^{206}Pb$ ages around 2 Ga (samples Bo1–1 and Bo1–4, Table 2) are probably close to the magmatic crystallisation age, concerning the magmatic feature of the zircons; thus they testify to the production of juvenile crust material during the Eburnean orogeny. The zircon ages between 2.5 and 2.6 Ga from assumed TTG reflect Latest Archean granite formation, which is a worldwide feature, or mixing ages. Anyhow, the 2.6-Ga age represents a minimum one for the inherited zircon cores of the studied sample.

The study area belongs to the West Central African Belt (WCAB), which resulted from the Eburnean collision between the Congo and São Francisco Cratons, and which is present as septa in the Late Neoproterozoic Panafrican Belt [41]. The main

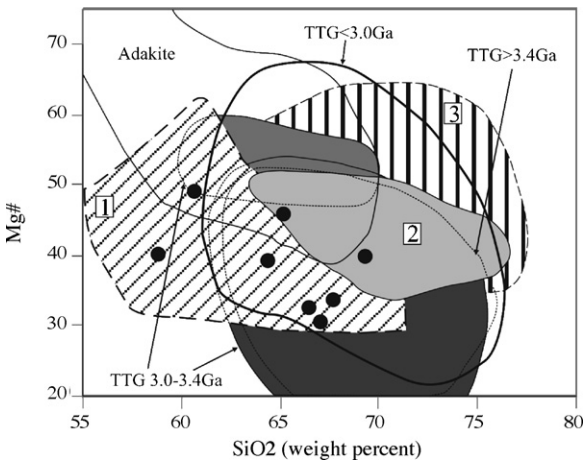

Fig. 7. SiO_2 versus Mg# (Mg number) diagram of studied gneisses in comparison with the Sangmelima TTG (**1**: charnockitic suite; **2**: tonalitic suite; **3**: granodiorite [48]) and other TTGs [51].

Fig. 7. Diagramme SiO_2 en fonction de Mg# (Mg number) des gneiss étudiés, en comparaison avec les TTG de Sangmelima (**1** : suite charnockitique ; **2** : suite tonalitique ; **3** : granodiorite [48]) et les champs de TTG de Smithies [51].

metamorphic event in the WCAB was dated at about 2050 Ma in the external zone (including the Nyong series) and 2100 Ma in the internal zone, the latter comprising the study area [41]. In the external zone, the metamorphic event was accompanied by emplacement of granodiorites (2066 Ma) and syenites (2055 Ma) [24]. We propose that the emplacement of the intrusive protolith of the pyroxene–amphibole-bearing gneiss occurred prior to the metamorphic event around 2.1 Ga, which then superimposed the gneissic structure to the rock.

The presence or influence of the Archean crust has been put into evidence in several regions in Nigeria [11]. The Kabba-Okenne granodiorite (widely occurring orthogneiss unit in the basement complex of Nigeria) gives a precise U–Pb zircon age of 2.1 Ga, which is interpreted as the crystallization age [2], but the Nd model age of 2.5 Ga in this granodiorite suggests that some Archean crustal component was incorporated when the Lower Proterozoic crust was formed [11]. Zircon Pb–Pb ages from an orthogneiss complex of the Caruaru area, northern Brazil, yielded crystallisation ages of 2.098 to 2.075 Ga [30]. Zircon U–Pb ages from orthogneisses north of the Pato shear zone, NE Brazil, reflect the 2.2–2.0-Ga Palaeoproterozoic crust, with local preservation of an Archean domain [60]. The Sm–Nd ages of 2.0 to 3.0 Ga in the Sertânia metasedimentary complex in the Alto Moxotó belt portray its provenance from Palaeoproterozoic and Archean sources [6].

The geochemical affinity of the studied gneisses with the Archean rocks (i.e. Sr/Y ratio, Y and REE contents) shows the inheritance of an older crustal signature during the emplacement of the protolith of the pyroxene–amphibole-bearing gneiss. The $^{207}Pb/^{206}Pb$ evaporation age around 2.0 Ga might be close to the crystallisation age, whilst the oldest age (2.6 Ga) probably represents a minimum age for the inherited zircon cores. Such cores could represent xenocrysts older than the gneiss protolith, which were incorporated into the melt during formation or emplacement. The zircon cores regularly show a round shape that might be due to their detrital origin. Such grains cannot be formed by magmatic precipitation in the original gneiss protolith. The detrital nature of the zircon cores provides evidence of the presence of older formations prior to the emplacement of the magmatic protolith of the pyroxene–amphibole-bearing gneiss.

The Archean zircon age (2.6 Ga) is the first Archean age obtained by the $^{207}Pb/^{206}Pb$ evaporation method in the Palaeoproterozoic septa of the Panafrican fold belt to the north of the Congo Craton in Cameroon. Archean inheritances had been demonstrated in the Panafrican fold belt by Nd model age or by upper intercept of U–Pb discordia ages. An amphibolite interlayered in the studied gneiss gave an Nd model age of 2.7 Ga [13]. In the Kombe area, in the southern part of the Panafrican fold belt in Cameroon, gneisses are characterized by Archean Nd model ages between 2.7 Ga and 3.5 Ga [12]. Archean ages (2.9 Ga) were also deduced from upper discordia intercepts (U–Pb) in many parts of the Panafrican fold belt [58], e. g., the Makenene, Kekem, and Kalaldi-Toldoro areas.

In the Nyong series, ages of 2.5 Ga to 2.6 Ga were obtained from pre orogenic sediments that had been submitted to the 2050 thermotectonic event [24]. The 2.4–2.6-Ga-old zircon cores in the studied gneiss probably derived from (meta)sediments deposited during the Palaeoproterozoic. This deposit was metamorphosed at ca. 2050 Ma during the Eburnean orogeny, which might have involved the entire West Central African Belt (WCAB). The studied gneiss belongs to an Eburnean–Transamazonian domain, which covers Central Africa and extends to northeastern Brazil.

Acknowledgements

The authors acknowledge Dr Hartmut Schulz for the CL images. The first author (AAG) is highly indebted to the German Academic Exchange Service (DAAD) for support of his research stay in the University of Tubingen. Frédéric Villeras of LEM (Nancy, France) is acknowledged for the REE analyses. Thanks go to two anonymous reviewers for their critical reviews of the manuscript.

References

[1] C. Allègre, Géologie isotopique, 2005, Belin.
[2] A.E. Annor, U–Pb Zircon age for Kabba–Okene granodiorite gneiss: implication for Nigeria's basement chronology, Afr. Geosci. Rev. 2 (1) (1995) 101–105.
[3] F. Barker, J.G. Arth, Generation of trondhjemitic–tonalitic liquids and Achaean bimodal trondhjemites-basalt suites, Geology 4 (1976) 596–600.
[4] B. Bessoles, M. Trompette, Géologie de l'Afrique : la chaîne Panafricaine, « Zone mobile d'Afrique centrale (partie sud) et Zone mobile soudanaise », Mem. BRGM, n°. 92, 1980.
[5] B. Bessoles, M. Lasserre, Le complexe de base du Cameroun, Bull. Soc. Geol. France (7) 19 (5) (1977) 1092–1805.
[6] B.B. Brito Neves, M.C. Campos Neto, W.R. Van Schmus, E.J. Santos, O 'sistema Pajeú–Paraíba' e o 'Maciço' São José do Campestre no l'este da Borborema, Rev. Bras. Geosci. 31 (2001) 173–184.
[7] C. Castaing, J.-L. Feybesse, D. Thiéblemont, C. Triboulet, P. Chèvremont, Paleogeographical reconstructions of the Pan-afri-

can/Brasiliano orogen: Closure of an oceanic domain or intracontinental convergence between major blocks? Precambr. Res. 69 (1994) 327–344.

[8] F. Chen, W. Siebel, M. Satir, Zircon U–Pb and Pb-isotope fractionation during stepwise HF-acid leaching and chronological implications, Chem. Geol. 191 (2002) 155–164.

[9] A. Cocherie, C. Guerrot, P. Rossi, Single-zircon dating by stepwise Pb evaporation: Comparison with other geochronological techniques applied to the Hercynian granites of Corsica, France, Chem. Geol. 101 (1992) 131–141.

[10] K.C. Condie, Archaen Greenstone Belts, Elsevier, New York, 1981.

[11] S.S. Dada, M.A. Rahaman, Archean and Lower Proterozoic crustal evolution in Nigeria, Afr. Geosci. Rev. 2 (2) (1995) 219–225.

[12] A.A. Ganwa, Contribution à l'étude géologique de la région de Kombé II–Mayabo dans la série panafricaine de Bafia : Géomorphologie structurale, tectonique, pétrologie, thèse de 3e cycle, université Yaoundé-1, 1998.

[13] A.A. Ganwa, Les granitoïdes de Méiganga : étude pétrographique, géochimique, structurale et géochronologique. Leur place dans la chaîne panafricaine. Thèse d'État ès sciences naturelles université Yaoundé 2005: (162 p.)

[14] J.B. Gill, Orogenic andesite and plate tectonic, in : P.J. Wyllie (Ed.), Minerals and Rocks, vol.16, Springer, Heidelberg, New York, 1981.

[15] B.M. Jahn, Z.Q. Zhang, Archaen granulite gneisses from eastern Hebei province, China: rare earth geochemistry and tectonic implications, Contrib. Mineral. Petrol. 85 (1984) 224–249.

[16] W.Q. Kennedy, The structural differentiation of Africa in Pan-African (500 Myr) tectonic episode, Sth. Ann. Rep. Res. Inst. African geol., University of Leeds, UK, 1964, pp. 1–48.

[17] U.S. Klötzli, Single zircon evaporation thermal ionisation mass spectrometry: Method and procedures, Analyst 122 (1997) 1239–1248.

[18] U.S. Klötzli, Th/U zonation in zircon derived from evaporation analysis: a model and its implications, Chem. Geol. 158 (1999) 325–333.

[19] B. Kober, Whole grain evaporation for $^{207}Pb/^{206}Pb$-age investigations on single zircons using a double-filament thermal ion source, Contrib. Mineral. Petrol. 93 (1986) 482–490.

[20] B. Kober, Single zircon evaporation combined with Pb + emitter bedding for $^{207}Pb/^{206}Pb$-age investigations using thermal ion mass spectrometry, and implications in zirconology, Contrib. Mineral. Petrol. 96 (1987) 63–71.

[21] A. Kröner, A.P. Willner, Time of formation and peak of Variscan HP–HT metamorphism of quartz-feldspar rocks in the central Erzgebirge, Saxony, Germany, Contrib. Mineral. Petrol. 132 (1998) 1–20.

[22] M. Lasserre, Carte géologique de reconnaissance à l'échelle 1/500 000, territoire du Cameroun, Ngaoundéré-Est, Dir. Mines Géol. Cameroun, Yaoundé, 1961 (1 carte et notice).

[23] R.W. Le Maitre, P. Bateman, A. Dudek, J. Keller, M.J. Lameyre, P.A. Le Bas, R. Sabine, H. Schmid, J. Sørenson, A. Streickeisen, A.R. Woolley, B. Zanettin, A Classification of Igneous Rocks and Glossary of terms, Blacwell, Oxford, UK, 1989.

[24] C. Lerouge, A. Cocherie, S.F. Toteu, J. Penaye, J.-P. Milési, R. Tchameni, E.N. Nsifa, C. Mark Fanning, E. Deloule, Shrimp U–Pb zircon age evidence for Paleoproterozoic sedimentation and 2.05-Ga syntectonic plutonism in the Nyong Group, southwestern Cameroon: consequences for the Eburnean–Transamazonian belt of NE Brazil and Central Africa, J. Afr. Earth Sci. 44 (2006) 413–427.

[25] W.F. McDonough, S.-S. Sun, The composition of the Earth, Chem. Geol. 120 (1995) 223–253.

[26] W.F. McDonough, S.-S. Sun, A.E. Ringwood, E. Jagoutz, A.W. Hofmann, Potassium, rubidium and cesium in the Earth and Moon and the evolution of the mantle of the Earth, Geochim. Cosmochim. Acta 56 (1992) 1001–1012.

[27] A. Nédélec, Late calcalkaline Plutonism in the Archean Ntem unit: the Sangmelima granodioritic suite (South Cameroon), Et. Rec. Geol. Afr. (1992) 25–28.

[28] A. Nédélec, J. Macaudière, J.-P. Nzenti, P. Barbey, Évolution structurale et métamorphique des schistes de Mbalmayo (Cameroun). Implication sur la structure de la zone mobile panafricaine d'Afrique centrale au contact du craton du Congo, C. R. Acad. Sci. Paris, Ser. II 303 (1986) 75–80.

[29] A. Nédélec, E.N. Nsifa, H. Martin, Major and trace element geochemistry of Achaean Ntem plutonic complex (South Cameroon): petrogenesis and crustal evolution, Precambr. Res. 47 (1990) 35–50.

[30] S.P. Neves, S.C. Melo, C.A.V. Moura, G. Mariano, J.M.R. Silva, Zircon Pb–Pb geochronology of the Caruaru area, northeastern Brazil: temporal constraints on the Proterozoic evolution of Borborema Province, Int. Geol. Rev. 46 (2004) 52–63.

[31] V. Ngako, Évolution métamorphique et structurale de la bordure sud-ouest de la série de Poli (segment Camerounais de la chaîne panafricaine), Mem. Centre. Arm. Et. Struct, socle, Rennes 5 (1986) 1–185.

[32] V. Ngako, P. Affaton, J.-M. Nnange, T. Njanko, Pan-African tectonic evolution in central and southern Cameroon; transpression and transtension during sinistral shear movements, J. Afr. Earth Sci. 36 (2003) 207–214.

[33] V. Ngako, P. Jégouzo, J.P. Nzenti, Champ de raccourcissement et cratonisation du Nord Cameroun du Protérozoïque moyen, C. R. Acad. Sci. Paris, Ser. II 315 (1992) 371–377.

[34] V. Ngako, P. Jégouzo et, D. Soba, Déformation et métamorphisme dans la chaîne Pan-africaine de Poli (Nord-Cameroun). Implications géodynamiques et paléogéographiques, J. Afr. Earth Sci. 9 (3/4) (1990) 541–555.

[35] I Ngounouno, Chronologie, pétrologie et cadre géodynamique du magmatisme cénozoique de la ligne du Cameroun, GEOCAM, 1/1998, Presses de l'université Yaoundé-1, pp. 169–184.

[36] J.-P. Nzenti, P. Barbey, J. Macaudière, D. Soba, Origin and evolution of the Late Precambrian high-grade Yaounde gneisses (Cameroon), Precambr. Res. 38 (1988) 91–109.

[37] J.-P. Nzenti, Pétrogenèse des migmatites de Yaoundé (Cameroun) : éléments pour un modèle géodynamique de la chaîne panafricaine Nord-équatoriale, thèse, université Nancy-1, 1987.

[38] J.-P. Nzenti, L'Adamaoua panafricain (région de Banyo) une zone clé pour un modèle géodynamique de la chaîne panafricaine nord-équatoriale au Cameroun, thèse d'État, université Cheick-Anta-Diop/université Nancy-1, 1994.

[39] J.T. O'Connor, A classification of quartz-rich igneous rocks based on feldspar ratios, US Geol. Surv. Prof. Pap. 525B (1965) 79–84.

[40] C.W. Passchier, J.S. Myers, A. Kröner, Field geology of high-grade gneiss terrains, Springer-Verlag, Berlin, Heidelberg, 1990.

[41] J. Penaye, S.F. Toteu, W.R. Van Schmus, J. Tchakounté, A. Ganwa, D. Minyem, E.N. Nsifa, The 2.1-Ga West Central African Belt in Cameroon: extension and evolution, J. Afr. Earth Sci. 39 (2004) 159–164.

[42] J. Penaye, S.F. Toteu, W.R. Van Schmus, J.P. Nzenti, U–Pb and Sm–Nd preliminary data on the Yaoundé series, Cameroon: reinterpretation of the granulitic rocks as the suture of a collision in the 'Centrafrican belt', C. R. Acad. Sci. Paris, Ser. II 317 (1993) 789–794.

[43] J. Penaye, S.F. Toteu, A. Michard, J.-M. Bertrand, D. Dautel, Reliques granulitiques d'âge Protérozoïque inférieur dans la zone mobile panafricaine d'Afrique centrale au Cameroun. Géochronologie U–Pb sur zircons, C. R. Acad. Sci. Paris, Ser. II 309 (1989) 315–318.

[44] J. Penaye, Pétrologie et structure des ensembles métamorphiques au sud-est de Poli (Nord Cameroun) : rôles respectifs du socle protérozoïque inférieur et de l´accrétion crustale panafricaine, thèse, université Nancy-1, France, 1988.

[45] R.T. Pidgeon, Recrystallisation of oscillatory zoned zircon: some geochronological and petrological implications, Contrib. Mineral. Petrol. 110 (1992) 463–472.

[46] C.K. Shang, Geology, Geochemistry and Geochronolgy of Archean rocks from the Sangmelima Region, Ntem complex, NW Congo Craton, South Cameroon, PhD thesis, University of Tübingen, Germany, 2001.

[47] C.K. Shang, M. Satir, W. Siebel, E.N. Nsifa, H. Taubald, J.-P. Liegeois, F.M. Tchoua, TTG magmatism in the Congo craton; a view from major and trace element geochemistry, Rb–Sr and Sm–Nd systematics: case of the Sangmelima region, Ntem complex, southern Cameroon, J. Afr. Earth Sci. 40 (2004) 61–79.

[48] C.K. Shang, W. Siebel, M. Satir, F. Chen, J. Mvondo Ondoua, Zircon Pb–Pb and U–Pb systematics of TTG rocks in the Congo Craton: Constraints on crust formation, magmatism, and Pan-African lead loss, Bull. Geosci. 79 (4) (2004) 205–219.

[49] J.W. Sheraton, K.D. Collerson, Geochemichal evolution of the Archean granulite facies gneisses in the westfold block and comparison with other gneiss complexes in the eastern Antartic shield, Contrib. Mineral. Petrol. 87 (1984) 61–64.

[50] W. Siebel, U. Blaha, F. Chen, J. Rohrmüller, Geochronology and geochemistry of a dyke–host rock association and implications for the formation of the Bavarian Pfahl shear zone, Bohemian Massif, Int. J. Earth Sci. (Geol. Rundsch.) 94 (2005) 8–23.

[51] R.H. Smithies, The Archean tonalite–trondhjemite–granodiorite (TTG) series is not and analogue of Cenozoic adakite, Earth Planet. Sci. Lett. 182 (2000) 115–125.

[52] G. Tagne-Kamga, Petrogenesis of the Neoproterozoic Ngondo Plutonic complex (Cameroon, West Central Africa): a case of late-collisional ferro-potassic magmatism, J. Afr. Earth Sci. 36 (2003) 149–171.

[53] J. Tchakounté, Étude géologique de la région d'Etoundou-Bayomen dans la série métamorphique de Bafia : tectonique, géochimie, métamorphisme, thèse de 3^{e} cycle, université Yaoundé-1, 1999.

[54] R. Tchameni, Géochimie et géochronologie des formations de l'Archéen et du Paléoprotérozoïque du Sud Cameroun (groupe du Ntem, craton du Congo), thèse, université d'Orléans, 1997.

[55] R. Tchameni, E.N Nsifa, K. Mezger, Recyclage crustal à l'Archéen supérieur dans le craton du Congo : cas des granitoïdes potassiques d'Ebolowa, groupe du Ntem, GEOCAM, 1/1998, Presses de l'université Yaoundé-1, pp. 339–350.

[56] R. Tchameni, A. Pouclet, J. Penaye, A.A. Ganwa, S.F. Toteu, Petrography and geochemistry of the Ngaoundéré Pan-African granitoids in Central North Cameroon: Implications for their sources and geological setting, J. Afr. Earth Sci. 44 (2006) 511–529.

[57] S.F. Toteu, J.-M. Bertrand, J. Penaye, J. Macaudière, S. Angoua, P. Barbey, Cameroon: a tectonic keystone in the Pan-african network, in: J.F. Lewry, M.R. Stauffer (Eds.), The Early Proterozoic Trans-Hudson orogen of North America, Geol. Assoc. Canada, Spec. Pap. 37 (1991) 483–496.

[58] S.F. Toteu, W.R. Van Schmus, J. Penaye, A. Michard, New U–Pb and Sm–Nd data from North-Central Cameroon and its bearing on the Pre-Pan African history of central Africa, Precambr. Res. 67 (2001) 321–347.

[59] F.S. Toteu, Chronologie des grands ensembles structuraux de la région de Poli. Accrétion crustale dans la chaîne panafricaine du Nord Cameroun, thèse d'État, université Nancy-1, 1987 (197 p.).

[60] W.R. Van Schmus, B.B. Brito Neves, P. Hackspacher, M. Babinski, U/Pb and Sm/Nd geochronologic studies of eastern Borborema Province, northeastern Brazil: Initial conclusions, J. South Am. Earth Sci. 8 (1995) 267–288.

[61] G. Vavra, On the kinematics of zircon growth and its petrogenetic significance: a cathodoluminescence study, Contrib. Mineral. Petrol. 106 (1990) 90–99.

[62] J.R. White, B.W. Chappell, Ultrametamorphism and granitoids genesis, Tectonophysics 43 (1977) 7–22.

[63] M. Wiedenbeck, P. Alle, F. Corfu, W.L. Griffin, M. Meier, F. Oberli, A. Von Quadt, J.C. Roddick, W. Spiegel, Three natural zircon standards for U–Th–Pb, Lu–Hf, trace element and REE analyses, Geostand. Newslett. 19 (1995) 1–23.